Cellular/Molecular

The Organization of Mitochondrial Quality Control and Life Cycle in the Nervous System *In Vivo* in the Absence of PINK1

Swathi Devireddy, Alex Liu, Taylor Lampe, and Peter J. Hollenbeck

Department of Biological Sciences, Purdue University, West Lafayette, Indiana 47907

Maintenance of healthy mitochondria is crucial in cells, such as neurons, with high metabolic demands, and dysfunctional mitochondria are thought to be selectively degraded. Studies of chemically uncoupled cells have implicated PINK1 mitochondrial kinase, and Parkin E3 ubiquitin ligase in targeting depolarized mitochondria for degradation. However, the role of the PINK1/Parkin pathway in mitochondrial turnover is unclear in the nervous system under normal physiological conditions, and we understand little about the changes that occur in the mitochondrial life cycle when turnover is disrupted. Here, we evaluated the nature, location, and regulation of quality control *in vivo* using quantitative measurements of mitochondria in *Drosophila* nervous system, with deletion and overexpression of genes in the PINK1/Parkin pathway. We tested the hypotheses that impairment of mitochondrial quality control via suppression of PINK1 function should produce failures of turnover, accumulation of senescent mitochondria in the axon, defects in mitochondrial traffic, and a significant shift in the mitochondrial fission–fusion steady state. Although mitochondrial membrane potential was diminished by *PINK1* deletion, we did not observe the predicted increases in mitochondrial density or length in axons. Loss of PINK1 also produced specific, directionally balanced defects in mitochondrial transport, without altering the balance between stationary and moving mitochondria. Somatic mitochondrial morphology was also compromised. These results strongly circumscribe the possible mechanisms of PINK1 action in the mitochondrial life cycle and also raise the possibility that mitochondrial turnover events that occur in cultured embryonic axons might be restricted to the cell body *in vivo*, in the intact nervous system.

Key words: axonal transport; *Drosophila*; mitochondrial function; mitochondrial turnover; motor neurons; PINK1

Introduction

Neurons depend critically upon mitochondrial functions, such as aerobic ATP production, calcium homeostasis, and control of apoptosis. An additional issue in these large asymmetric cells is the compartmentalization of the different parts of the mitochondrial life cycle: biogenesis, transport, changes in metabolic state, fission–fusion, and turnover (Saxton and Hollenbeck, 2012). In neurons, as in other cells, these features appear to be performed in a coordinated fashion, commonly referred to as "mitochondrial quality control," to maintain a robustly functional mitochondrial population, minimizing the effects of somatic mtDNA mutations and protein damage (Chang and Reynolds, 2006; Chen and Chan, 2009; Rugarli and Langer, 2012). Although mitochondrial biogenesis, fission–fusion, and turnover may occur primarily in the cell body (CB), evidence from embryonic neu-

rons indicates that they can also occur in the axon (Amiri and Hollenbeck, 2008; Maday et al., 2012; Cagalinec et al., 2013). Furthermore, disruption of fission–fusion affects mitochondrial transport (Verstreken et al., 2005; Baloh et al., 2007; Misko et al., 2010), and vice versa (Pathak et al., 2010; Cagalinec et al., 2013). Moreover, mitochondrial axonal transport is affected by a variety of disruptions of mitochondrial metabolism (e.g., Hollenbeck et al., 1985; Rintoul et al., 2003; Miller and Sheetz, 2004). Thus, although the mechanisms remain unclear, it is apparent that disparate events in the mitochondrial life cycle are indeed closely interrelated.

Recent studies have suggested that mitochondrial quality control involves the Parkinson's disease-related PTEN-induced putative kinase 1 (PINK1) and Parkin (Clark et al., 2006; Park et al., 2006; Gautier et al., 2008). Evidence indicates that PINK1 retained on the surface of depolarized mitochondria recruits Parkin, which then tags the mitochondrion for autophagy (Matsuda et al., 2010; Narendra et al., 2010) and also stimulates degradation of Mitofusin, preventing the fusion of senescent mitochondria with "healthy" neighbors until they are turned over (Poole et al., 2010; Ziviani et al., 2010). PINK1 has also been proposed to regulate the mitochondrial transport by stimulating the turnover of the mitochondrion-kinesin linker protein Miro and thus immobilizing certain organelles (Wang et al., 2011). If these mechanisms operate in neurons, then we expect that the impairment of mitochondrial quality control via suppression of PINK1 function will produce several cellular phenotypes: failures of turnover, ac-

cumulation of senescent mitochondria in the axon, defects in mitochondrial traffic, and a significant shift in the mitochondrial fission–fusion steady state. Here we tested these hypotheses *in vivo*, using quantitative observations of mitochondria in *Drosophila* nervous system with deletion and overexpression of genes in the PINK1/Parkin pathway. Although we found diminished mitochondrial membrane potential in *PINK1* deletion, we did not observe the predicted increase in mitochondrial density or length in axons. In addition, loss of PINK1 caused more specific, essentially balanced defects in mitochondrial transport, without altering the balance between stationary and moving mitochondria. These results circumscribe the possible mechanisms of PINK1 action in the mitochondrial life cycle and also raise the possibility that mitochondrial turnover events that occur in cultured embryonic neurons might be restricted to the CB *in vivo*, in the intact nervous system.

Materials and Methods

Drosophila stocks. All fly stocks (w^{1118}, D42-Gal4>UAS-mitoGFP, $PINK1^{RV}$, $PINK1^{B9}$/FM7GFP;D42>UAS-mitoGFP/TM6C, Casper Pink1-Myc, UAS-PINK1/CyO;TM6B/MKRS, UAS-Parkin/CyO, $PINK1^5$/FM7GFP;D42>UAS-mitoGFP/TM6C, $PINK1^9$/FM7GFP;D42>UAS-mitoGFP/TM6C, UAS-NDI1) were maintained in standard cornmeal agar medium with a 12 h light-dark cycle and 50%–55% humidity at 25°C. Only *PINK1* mutant males were obtained from the maintenance of sterile *PINK1* mutants over X chromosome balancer, and only male larvae were used for all the experiments, except for $PINK1^5$/+ heterozygous female larvae. The above fly stocks were used in specific crosses to obtain larvae of the following genotypes for use in experiments: **Wild-type** (+/Y;;D42>UAS-mitoGFP/+), $\mathbf{PINK1}^{RV}$ ($PINK1^{RV}$/Y;;D42>mitoGFP/+): control for $PINK1^{B9}$, $\mathbf{PINK1}^{B9}$ ($PINK1^{B9}$/Y;;D42>mitoGFP/+), $\mathbf{PINK1}^5$/+ ($PINK1^5$/+;;D42>mitoGFP/+): heterozygous control for $PINK1^5$, $\mathbf{PINK1}^5$ ($PINK1^5$/Y;;D42>mitoGFP/+), **B9;P(Pink1)** ($PINK1^{B9}$/Y;;D42>mitoGFP/Casper Pink1-Myc), $\mathbf{PINK1}^5$**;P(Pink1)** ($PINK1^5$/Y;;D42>mitoGFP/Casper Pink1-Myc), **B9;Parkin OE** ($PINK1^{B9}$/Y;UAS-Parkin/+;D42>mitoGFP/+), $\mathbf{PINK1}^5$**;Parkin OE** ($PINK1^5$/Y;UAS-Parkin/+;D42>mitoGFP/+), **PINK1 OE(1)** (+/Y;UAS-PINK1/+;D42>mitoGFP), **PINK1 OE(2)** (+/Y;UAS-PINK1/UAS-PINK1;D42>mitoGFP), **Parkin OE(1)** (+/Y;UAS-Parkin/+;D42>mitoGFP), **B9;NDI1 OE** ($PINK1^{B9}$/Y;UAS-NDI1/+;D42>mitoGFP/+), $\mathbf{PINK1}^5$**; NDI1 OE** ($PINK1^5$/Y;UAS-NDI1/+;D42>mitoGFP/+). For analysis of percentage of moving mitochondria and mitochondrial lengths in axons, we used wild-type control, $PINK1^{B9}$, $PINK1^5$, $PINK1^9$, PINK1 OE(1), PINK1 OE(2), and Parkin OE(1) expressing UAS-mitoGFP in two copies (D42>UAS-mitoGFP/D42>UAS-mitoGFP).

Dissected larval preparation for live cell confocal imaging. Wandering late third instar larvae were partially dissected in HL6 buffer containing 0.6 mM CaCl₂ and 4 mM L-glutamate, by longitudinally incising the dorsal body wall and gently removing the intestine and fat bodies to reveal the ventral ganglion and intact segmental nerves (SNs) attached to the larval body wall (Pilling et al., 2006; Louie et al., 2008; Shidara and Hollenbeck, 2010; Devireddy et al., 2014). The dissected larva was gently placed on a glass slide, covered with a cover glass using double-sided tape as a spacer, and sealed with VALAP on either side to form a chamber. The whole imaging process was then completed within 25 min to ensure normal physiological conditions of the live nervous system. All imaging was performed using a 60× oil-immersion objective with the Nikon C-1 laser scanning confocal system mounted on a Nikon Eclipse 90i microscope with EZ-C1 and Elements software.

Determination of mitochondrial inner membrane potential (IMP or $\Delta\psi_m$). The larval preparation was treated with 200 nM tetramethylrhodamine methyl ester (TMRM, Invitrogen; catalog #T668) in HL6 buffer for 30 min, followed by imaging in 50 nM TMRM. Confocal images of neuromuscular junctions 6/7 (NMJs 6/7) and thin neurons adjacent to SNs in A4 abdominal segment were acquired sequentially with 488 nm and 561 nm lasers for mitoGFP and TMRM, respectively. The TMRM images of neurons were thresholded using ImageJ to isolate mitochondrial pixels and determine the mitochondrial fluorescence intensities

(F_m), and then adjacent cytoplasmic fluorescence intensities (F_c) were determined using hand-drawn regions. The ratio of mitochondrial to cytoplasmic fluorescence (F_m/F_c) was used as a measure of mitochondrial membrane potential ($\Delta\psi_m$) in axons (Verburg and Hollenbeck, 2008; Shidara and Hollenbeck, 2010). $\Delta\psi_m$ at NMJs was determined by quantifying the mean mitochondrial intensities (F_m) from thresholded TMRM images (Shidara and Hollenbeck, 2010).

Analysis of mitochondrial motility. For mitochondrial motility analysis, time lapse confocal images of mitoGFP were acquired in middle (A4) region of the longest SN in the larva with a 488 nm laser (5%; 150 mW laser power) and a 30 µm pinhole at 1 frame/s for 5 min (Nikon, Eclipse 90i). Mitochondrial motility parameters, such as flux (number of moving through the axon per unit time), duty cycles (percent time mitochondria spend in their primary direction runs, reverse runs, and pauses), and run velocities, were quantified as previously described using the manual tracking plugin of ImageJ (Pilling et al., 2006; Shidara and Hollenbeck, 2010; Devireddy et al., 2014). Kymographs were prepared from the time lapse images, by using the Image/ND processing/Create kymograph by line option in Nikon NIS-Elements software.

Quantitation of percentage moving mitochondria, mitochondrial density, and mitochondrial lengths in SNs. To quantify the percentage of moving mitochondria in SNs, time lapse images were acquired at 1 frame/2 s for 2 min. Mitochondria present in the first frame were only considered while counting the stationary and moving mitochondria, due to the varied number of moving mitochondria entering the field of view over time. Mitochondria were categorized as anterograde, retrograde, stationary (remaining at the same position during the imaging period), or oscillating (moving back and forth with an amplitude ≤ 5 µm without significant net displacement). To determine mitochondrial density, the first frame from the time lapse image sequence was thresholded and binarized to obtain number of mitochondrial pixels per length of the segmental nerve. Mitochondrial lengths were measured using the Feret's diameter option in the ImageJ/Analyze menu on thresholded, binarized images. Where mitochondrial edges were not distinct enough, the Watershed function was used on binarized images to separate these adjoined mitochondria, before measuring their lengths.

Imaging and quantitation of mitochondria in CBs. Confocal Z-stacks of CBs (with slice thickness 0.15 µm) were acquired of the larval ventral ganglion using a 60× oil-immersion Nikon objective. The stacks were aligned with the ImageJ/Stackreg plugin (Thevenaz et al., 1998), using the middle slice as an anchor, to eliminate the effects of drift. CBs with large, round mitochondria of sizes >2 µm² were counted, and their areas were measured by drawing a Polyline around them in a Z-slice where they were in sharp focus. Mitochondrial volume was determined in CBs by setting the intensity threshold on Z-slices using 3D object counter (Bolte and Cordelières, 2006) and 3D ROI manager (Ollion et al., 2013) plugins in ImageJ.

Statistics. For all experiments, the number of larvae (n) analyzed is represented in graphs, and error bars indicate mean ± SEM. All statistical comparisons were performed between wild-type versus *PINK1* mutants and mutants versus mutants with PINK1 or Parkin expression in GraphPad Prism, using one-way ANOVA with Bonferroni's post-test (for normally distributed data); otherwise, the nonparametric Kruskal–Wallis test followed by Dunn's post-test was used (for non-normally distributed data). For the analysis of mitochondrial length distributions, a nonparametric two-sample Kolmogorov–Smirnov (KS) test was performed (Siegel and Castellan, 1988).

Results

Neurons show diminished mitochondrial inner membrane potential (IMP or $\Delta\psi_m$) in the absence of PINK1

Evidence for PINK1 involvement in the turnover of damaged or depolarized mitochondria comes from studies of chemically uncoupled cultured cells (Matsuda et al., 2010; Narendra et al., 2010), along with analyses of mitochondrial morphology (Clark et al., 2006; Park et al., 2006) and biochemical activity (Morais et al., 2009) in *Drosophila PINK1* mutants. A strong prediction of the model derived from these and other
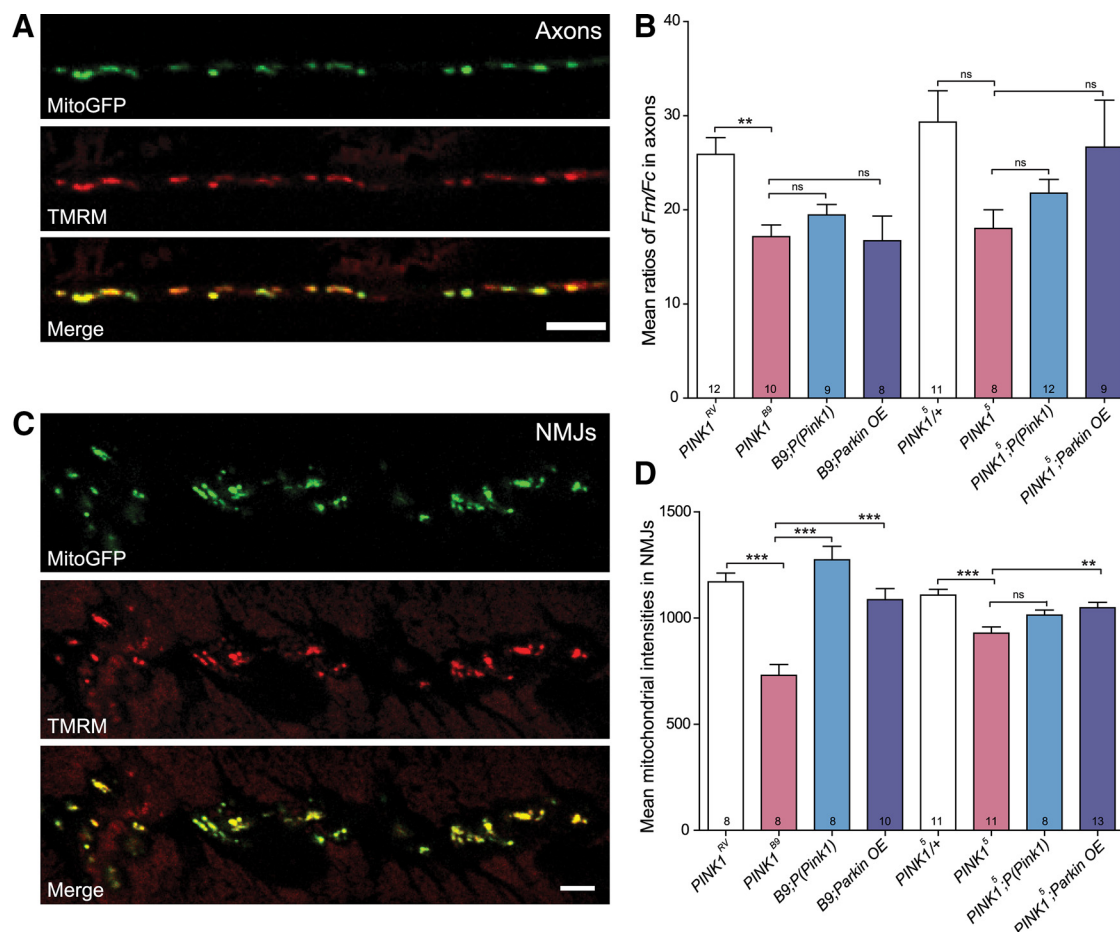
Figure 1. Neurons of *PINK1* mutants show reduced mitochondrial IMP or $\Delta\psi_m$. **A, C,** TMRM staining of mitochondria (red) reveals the mitochondrial membrane potential ($\Delta\psi_m$), whereas MitoGFP (green) is used to identify mitochondria in axons (**A**) and NMJs (**C**) of *Drosophila* larval motor neurons in segmental nerves. Merge (yellow) shows the colocalization of MitoGFP- and TMRM-stained mitochondria. These images show *PINK1^{RV}* control larvae. Scale bar, 5 μm. Mean F_m/F_c intensity ratios of TMRM in axons (**B**) and mean F_m intensities of TMRM in NMJs (**D**) are quantified for *PINK1^{RV}* control, *PINK1^{B9}*, *PINK1^{B9};P(Pink1)* (genomic rescue), and *PINK1^{B9};Parkin OE* and for *PINK1^5/+* control, *PINK1^5*, *PINK1^5;P(Pink1)* (genomic rescue), and *PINK1^5;Parkin OE*. Compared with control larvae, *PINK1* mutants show a decrease in mean TMRM intensities, which is rescued significantly in NMJs by expression of P(Pink1) and Parkin overexpression (OE) but improved only modestly in *PINK1^5* mutant axons. Error bars indicate SEM; number of larvae is represented on graph bars. Ten to 20 mitochondria were quantified per larva. **p < 0.01, ***p < 0.001 (one-way ANOVA with Bonferroni's post-test). ns, Nonsignificant differences.

studies (Youle and Narendra, 2011; Ashrafi and Schwarz, 2013) is that loss of PINK1 should cause accumulation of senescent mitochondria with diminished mitochondrial membrane potential ($\Delta\psi_m$) in axons. To test this hypothesis *in vivo*, we first assessed the $\Delta\psi_m$ of mitochondria in neurons of the intact *Drosophila* nervous system. To a filleted larval preparation (Pilling et al., 2006; Shidara and Hollenbeck, 2010; Devireddy et al., 2014), we applied TMRM, a lipophilic cationic fluorescent dye, which equilibrates between the cytoplasm and the mitochondrial matrix based on the magnitude of the $\Delta\psi_m$ (Fig. 1*A,C*) (Scaduto and Grotyohann, 1999; Verburg and Hollenbeck, 2008). We quantified the ratio of mitochondrial to cytoplasmic fluorescence intensities (F_m/F_c), which is related logarithmically to $\Delta\psi_m$ in axons (Verburg and Hollenbeck, 2008; Shidara and Hollenbeck, 2010). We observed a reduction in the mean F_m/F_c values in motor axons and mean F_m values in NMJs of *PINK1* mutants (*PINK1^{B9}* or *PINK1^5*) compared with control, as expected (Fig. 1*B,D*). This deficit is partially rescued in NMJs of *PINK1* mutants by expressing physiological levels of *PINK1* from a genomic promoter (Clark et al., 2006) (Fig. 1*B,D*). Because the ubiquitin ligase Parkin has been shown to act downstream in the PINK1 mitochondrial maintenance pathway (Clark et al., 2006; Park

et al., 2006), we also assessed the IMP in *PINK1* mutants with Parkin overexpression and observed significant rescue of IMP in NMJs (Fig. 1*D*) and a trend toward rescue in *PINK1^5* mutant axons (Fig. 1*B*). In *PINK1* mutants, either expressing PINK1 at genomic levels or overexpressing Parkin rescued the mitochondrial IMP in NMJs, but did not in axons, suggesting that the roles of PINK1 and Parkin in maintaining mitochondrial function differ by region, perhaps in relation to specific bioenergetic demands of different compartments (Hollenbeck, 2005; Hollenbeck and Saxton, 2005).

Mitochondrial axonal transport is impaired in the absence of PINK1

Because most mitochondrial turnover in neurons is thought to occur in the CB (Cai et al., 2012; Saxton and Hollenbeck, 2012), another prediction of PINK1 involvement in mitochondrial turnover is that reduced PINK1 function should cause the accumulation of senescent mitochondria in the axon, through a reduction in their retrograde retrieval and turnover. To examine this, we quantified mitochondrial axonal transport in motor axons of middle segmental nerves (A4) of *Drosophila* larvae by tracking individual mitochondria on the time lapse images (Shidara and Hollenbeck, 2010; De-
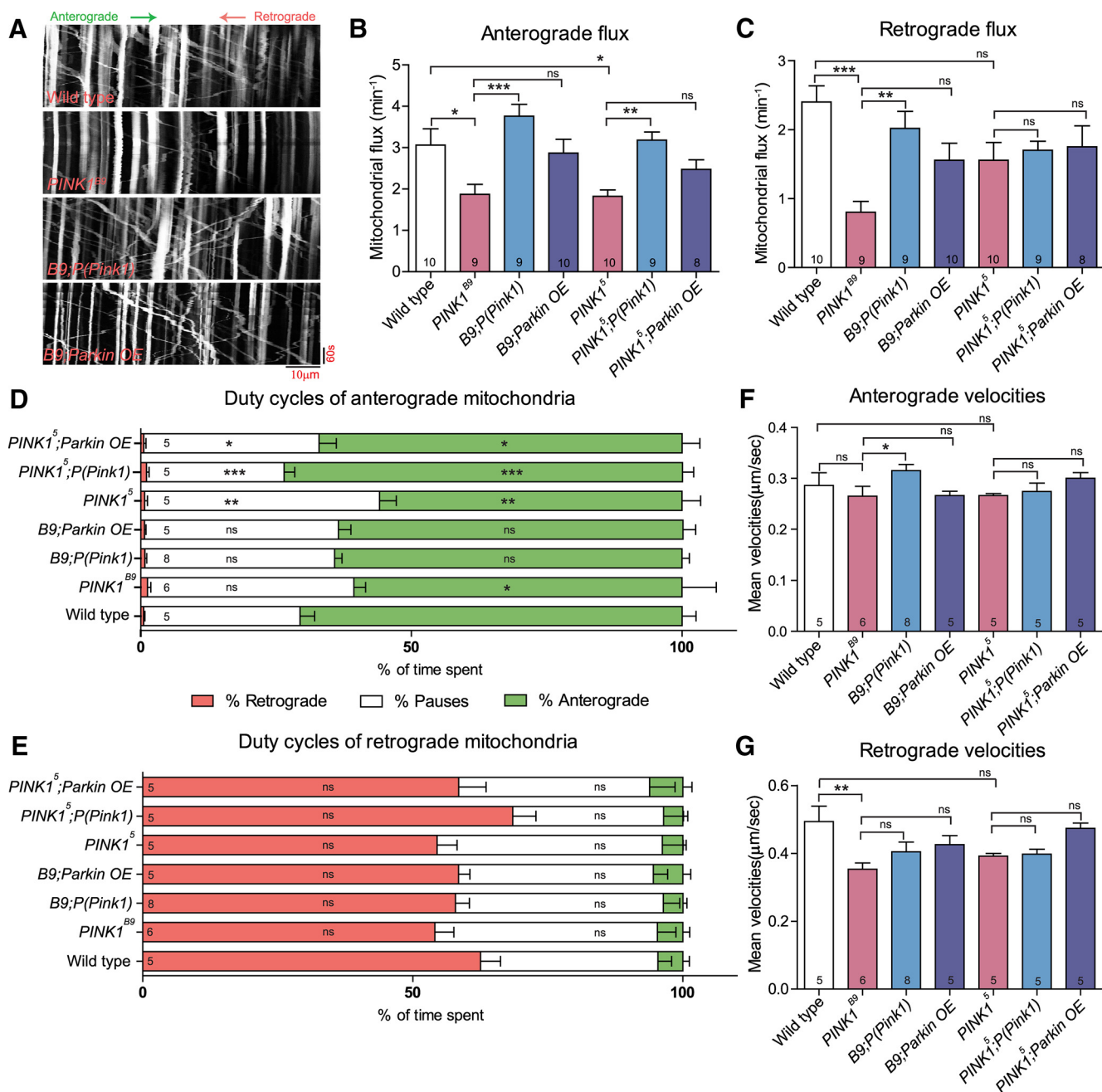
Figure 2. *PINK1* mutants show bidirectional mitochondrial motility changes with reduced flux and reduced anterograde duty cycles. **A,** Kymographs of axonal mitochondrial transport in segmental nerves of wild-type, *PINK1B9*, *PINK1B9;P(Pink1)* (genomic rescue), and *PINK1B9;Parkin OE,* displaying 5 min of movement; anterograde movement is toward the right. Vertical lines indicate stationary mitochondria. Scale bar, 10 μm. **B, C,** *PINK1* mutants show reduced flux in both anterograde (**B**) and retrograde (**C**) directions. This is rescued by expression of P(Pink1) and is partially rescued by Parkin overexpression. **D, E,** *PINK1* mutants show reduced duty cycles for anterograde mitochondria, with more time spent in pauses and less time moving in their primary anterograde direction (**D**). However, duty cycles of retrograde mitochondria are unchanged by loss of PINK1 (**E**). **F, G,** Mean run velocities of retrograde (**G**), but not anterograde (**F**), mitochondria are reduced in the absence of PINK1. The number of larvae analyzed for different genotypes is indicated on each bar. Each larval mean was calculated by averaging the values of at least five mitochondria for each direction, and tests were performed on the means of the larval means. Error bars indicate SEM. One-way ANOVA with Bonferroni's post-test was used for normally distributed data. Kruskal–Wallis with Dunn's post-test was used for non-normally distributed data. *$p < 0.05$, **$p < 0.01$, ***$p < 0.001$. ns, Nonsignificant differences.

vireddy et al., 2014). In axons of segmental nerves, anterograde and retrograde populations of mitochondria are clearly distinguished from each other by their preferential movement in the dominant direction, with a smaller fraction of their time spent pausing, and a very small fraction spent reversing direction; this can be seen in kymographs (Fig. 2A). A detailed quantification of motility (Fig. 2B,C) showed that mitochondrial flux was indeed reduced in both the anterograde and retrograde directions in *PINK1* mutants compared with wild-

type, and this was rescued significantly by the expression of *PINK1* by a genomic promoter and partially by overexpression of Parkin (Fig. 2B,C).

To understand the specific changes in mitochondrial motility behavior that caused reduced flux, we quantified the duty cycles and velocities of the moving mitochondrial population in axons of wild-type and *PINK1* mutants. In wild-type, anterograde mitochondria spent ~70% time in anterograde runs, ~29% in pauses, and ~1% in retrograde runs. In the absence of PINK1,
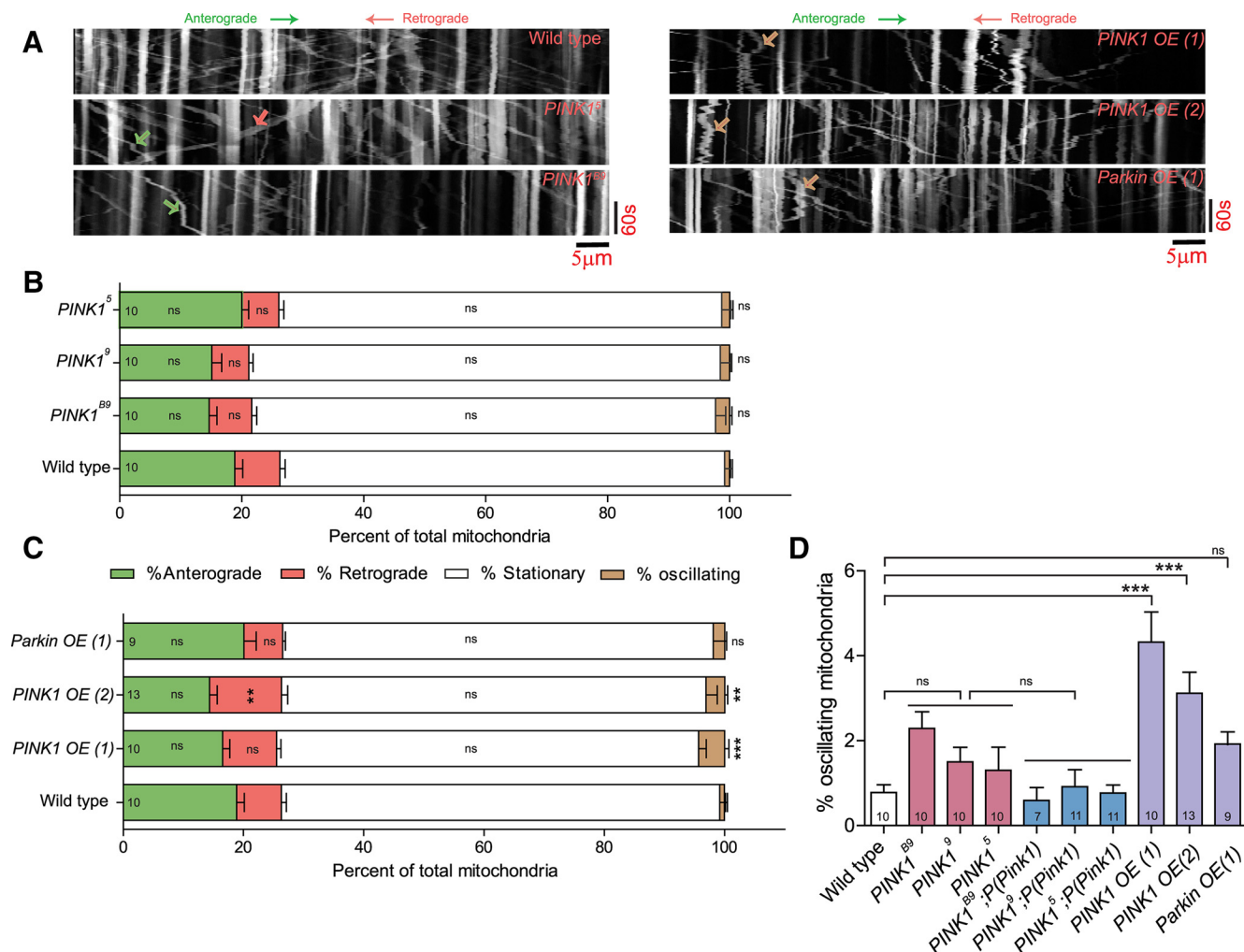
Figure 3. Balance of moving and stationary mitochondria in PINK1 loss of function and overexpression conditions. ***A***, Kymographs of axonal mitochondrial motility in A4 segmental nerves of wild-type, *PINK1⁵*, *PINK1^B9^*, *PINK1 OE(1)*, *PINK1 OE(2)*, and *Parkin OE(1)*, displaying 2 min of movement; anterograde movement is toward the right. Vertical lines indicate stationary mitochondria. Arrows indicate the movement of anterograde mitochondria (green), retrograde mitochondria (red) in *PINK1* mutants, and oscillatory movements of mitochondria (brown) in *PINK1 OE* and *Parkin OE*. Scale bar, 5 μm. ***B***, In wild-type segmental nerves, ∼72% of mitochondria are stationary, with ∼20% moving anterogradely and ∼10% moving retrogradely. None of the *PINK1* mutants showed a significant difference in percentage of either stationary or moving (anterograde, retrograde) mitochondria. ***C***, Single-copy overexpression of *PINK1 OE(1)* and *Parkin OE(1)* also produces no change in the fraction of stationary mitochondria, whereas two-copy overexpression of *PINK1 OE(2)* actually increases the percentage of retrogradely moving mitochondria. ***D***, Oscillating mitochondria, observed rarely in wild-type (∼1%), increase significantly to ∼3%-4% in *PINK1 OE(1)* and *PINK1 OE(2)*. Number of larvae analyzed is indicated on each bar. Error bars indicate SEM. **p < 0.01, ***p < 0.001 (one-way ANOVA with Bonferroni's post-test). ns, Nonsignificant differences compared with wild-type (***B–D***) and *PINK1;P(Pink1)* compared with *PINK1* mutants (***D***).

anterograde mitochondria showed a significant reduction in percentage of time in anterograde runs (55%–60%), resulting in an increase in percentage of time in pauses (38%–44%); however, there was no change in retrograde runs (∼1%) (Fig. 2*D*). These defects in duty cycles of anterograde mitochondria were ameliorated by expressing *PINK1* with a genomic promoter or by Parkin overexpression. However, duty cycles of retrograde mitochondria were only modestly affected in *PINK1* mutants compared with wild-type (Fig. 2*E*). In addition, the anterograde velocities were not affected (Fig. 2*F*), but retrograde velocities were reduced by the loss of PINK1, compared with wild-type (Fig. 2*G*). Thus, the reduction in anterograde flux observed in the absence of PINK1 results in large part from a reduced anterograde duty cycle, whereas the small reduction in retrograde flux can be explained by reduced velocities. The net loss of retrograde retrieval predicted by the proposed PINK1 role in mitochondrial turnover is not observed here.

Fractions of stationary and moving mitochondria remain unaffected in the absence of PINK1 or in PINK1 overexpression conditions

Another way in which mitochondrial flux in the axon could be modulated by the PINK1 pathway would involve the recruitment between persistently stationary and mobile populations (Saxton and Hollenbeck, 2012; Devireddy et al., 2014). Indeed, it has recently been proposed that PINK1 stops the movement of depolarized mitochondria by degrading Miro, a kinesin-mitochondria adaptor protein (Wang et al., 2011; Liu et al., 2012). Thus, we analyzed the total mitochondrial population in motor axons of SNs to determine whether the loss or overexpression of PINK1 altered the fractions of moving and persistently stationary mitochondria. In wild-type nerves, the majority of axonal mitochondria are stationary (72.9 ± 1.2%; mean ± SEM); and of the 26% that are moving, 18.8 ± 1.3% move anterogradely and 7.4 ± 0.9% move retrogradely (Fig. 3*A,B*). In *PINK1* mutants, by com-
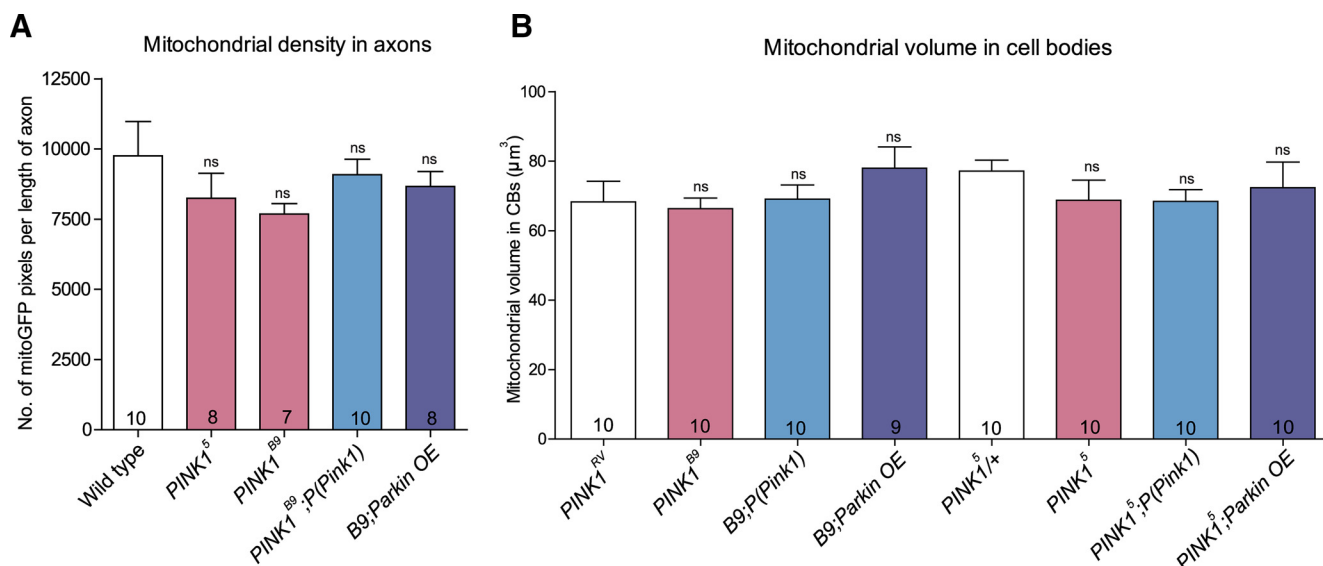
A

B

Figure 4. PINK1 loss does not lead to accumulation of mitochondria to higher densities in axons or CBs. ***A***, Loss of PINK1 does not result in an increase in mitochondrial density in motor axons. ***B***, Mitochondrial density in motor neuron CBs also remains unchanged in *PINK1* mutants compared with *PINK1^RV^* control for *PINK1^B9^* and *PINK1^5^/+* control for *PINK1^5^*. Number of larvae analyzed is indicated on each bar. Error bars indicate SEM; one-way ANOVA with Bonferroni's post-test, all are nonsignificant (ns); mutants compared with wild-type or control and *PINK1;P(Pink1)* or *PINK1;Parkin OE* compared with *PINK1* mutants.

parison, we did not observe any significant change in distribution between the moving or stationary populations (Fig. 3*B*). Furthermore, overexpression of PINK1 or Parkin in a single copy had modest or no effects on either stationary or moving mitochondrial numbers, whereas overexpression of PINK1 in two copies actually caused an increase in the retrograde population only (Fig. 3*C*). These data suggest that the balance between the persistently moving and stationary mitochondrial populations is virtually unaffected by PINK1 levels, even though mitochondrial motility behavior is affected by PINK1 loss. We did observe a significant increase in the small fraction of oscillating mitochondria (from <1% to 4.3% of total mitochondria) in motor axons when either PINK1 or Parkin was overexpressed (Fig. 3*A,D*). A similar motility phenotype has been observed previously in regions of vertebrate axons focally stimulated with nerve growth factor; there, it was attributed to the initiation of static docking interactions between mitochondria and the actin cytoskeleton in response to signaling (Chada and Hollenbeck, 2003, 2004).

Mitochondrial density is not increased in the absence of PINK1

The observed alteration in mitochondrial flux in *PINK1* mutants could also result in part from a change in the overall density of mitochondria in the axons. Indeed, a prediction of the PINK1 model of mitochondrial quality control (Youle and Narendra, 2011; Ashrafi and Schwarz, 2013) is that defective turnover should cause senescent mitochondria to accumulate in *PINK1* mutant axons. Thus, we determined whether the loss of PINK1 causes an increased mitochondrial density in larval SN axons. Interestingly, we observed no significant change in the *PINK1* mutants compared with wild-type (Fig. 4*A*). This result could be explained if most mitochondrial quality control and turnover processes were localized to CBs. We therefore determined the mitochondrial density in motor CBs of the ventral ganglion using 3D reconstruction of confocal images and found that, here too, the mitochondrial density was very similar between *PINK1* mutants and wild-type animals, giving no indication of accumulation of senescent organelles (Fig. 4*B*).

Loss of PINK1 causes mitochondrial morphology defects in motor CBs, but not in motor axons

Because PINK1 has been proposed to inhibit the fusion of damaged with healthy mitochondria via degradation of the fusion protein dMfn (Poole et al., 2010; Ziviani et al., 2010), another prediction of the PINK1/Parkin model of mitochondrial quality control is that *PINK1* mutants should accumulate longer mitochondria. In motor axons of wild-type larva (Fig. 5*Ai*), we observed that stationary mitochondria (mean = 1.3 ± 0.04 μm) were not significantly longer than moving mitochondria (anterograde, 1.21 ± 0.04 μm; retrograde, 1.24 ± 0.09 μm). However, *PINK1* mutants showed no significant difference in the mean lengths of either their stationary or moving mitochondria (Fig. 5*Aii,B–D*). Deficient inhibition of fusion could also result in a small outlying population of longer organelles not detectable as a difference in means, so we compared the frequency distribution of lengths. Despite the appearance of a slight skew toward longer categories in *PINK1* mutants, we found no statistically significant difference in the length distribution (Fig. 5*E*) (ns, nonparametric two-sample KS test). Thus, loss of PINK1 function did not result in detectable accumulation of longer mitochondria in motor axons. Nonetheless, overexpression of PINK1 (Fig. 5*Aiii*) significantly reduced the mean lengths of stationary mitochondria (1.11 ± 0.02 μm) (Fig. 5*B*), without affecting the mean lengths of moving mitochondria (Fig. 5*C,D*). Analysis of the stationary length distribution also showed more small mitochondria in PINK1 overexpression compared with wild-type (Fig. 5*E*) (*p* < 0.001, nonparametric two-sample KS test). These results suggest that overexpression of PINK1, but not its loss, affected mitochondrial morphology in motor axons.

However, mitochondrial morphology in motor CBs was indeed affected by PINK1 loss. Whereas mitochondria were organized as a filamentous reticulum in motor CBs in the ventral ganglion of wild-type larvae (Fig. 6*Ai,Avi*), in *PINK1* mutants, we observed a subset of much larger, rounder, discrete mitochondria (Fig. 6*Aii,Avii*, arrows). We quantified the percentage of CBs with these abnormally large mitochondria (defined as having an area of >2 μm² in 2D projection) and found that the loss of PINK1
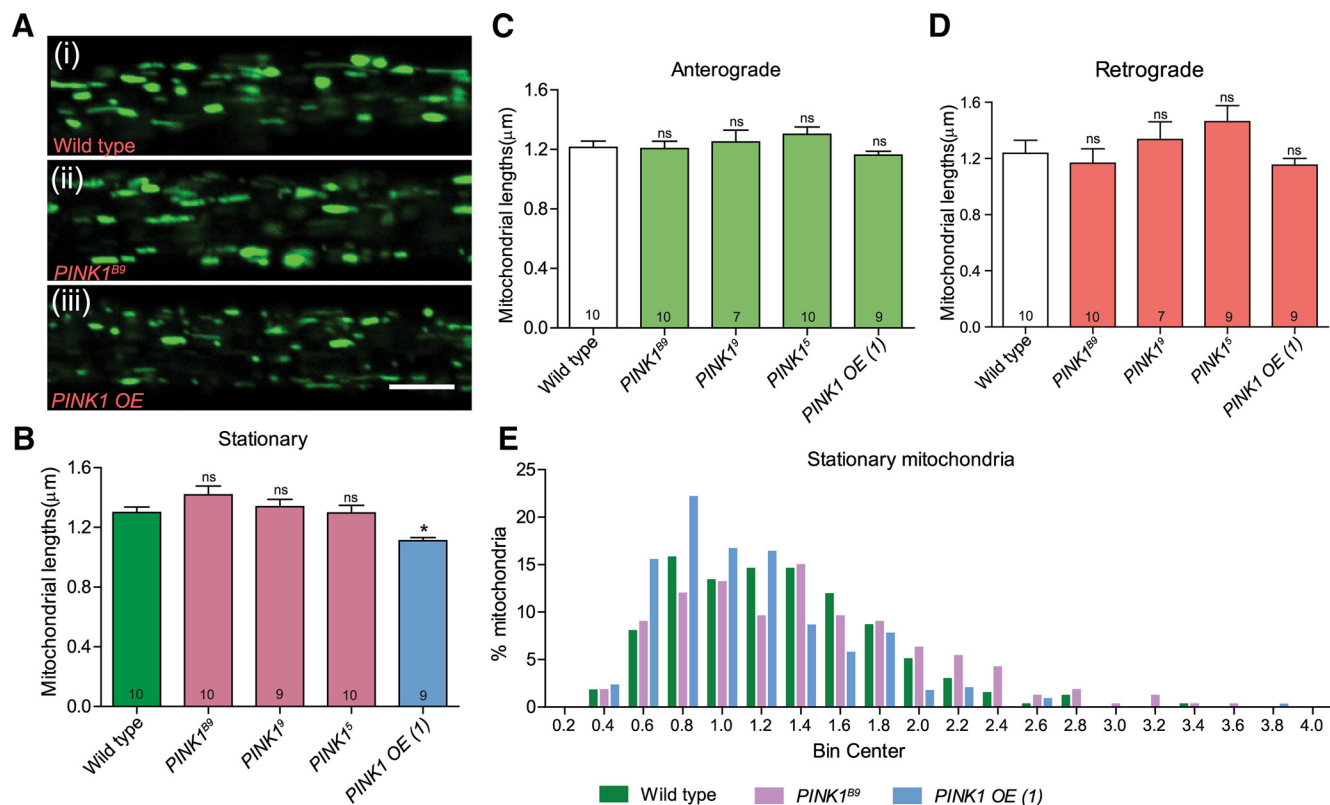
Figure 5. PINK1 loss does not shift fission–fusion balance toward longer axonal mitochondria. ***A***, Mitochondria in the axons of wild-type (***i***), *PINK1^B9* mutant (***ii***), and PINK1 OE(1) (***iii***). Scale bar, 5 μm. Mean lengths of stationary (***B***), anterograde (***C***), and retrograde (***D***) mitochondria are determined for wild-type, *PINK1* mutants, and PINK1 OE(1). Only PINK1 OE(1) produces a change, and this is a decrease in mean lengths of stationary (***B***) mitochondria. ***E***, Frequency distribution of stationary mitochondrial lengths was analyzed for wild-type, *PINK1^B9*, and PINK1 OE(1). Number of larvae analyzed is shown on each bar. Error bars indicate SEM. *$p < 0.05$ (nonparametric Kruskal–Wallis test followed by Dunn's post-test). ns, Nonsignificant values compared with wild-type (***B–D***). Nonparametric two-sample KS test for frequency distribution (***E***), $p < 0.001$ for wild-type versus PINK1 OE(1) and nonsignificant for wild-type versus *PINK1^B9*.

caused the formation of these abnormal mitochondria in ∼60% of the CBs observed (Fig. 6B) compared with only 8% in controls type. Normal mitochondrial morphology was significantly restored by the expression of genomic levels of PINK1 or by the overexpression of Parkin (Fig. 6B). These data suggest that mitochondrial morphology is altered in CBs in the absence of PINK1 function, probably due to defects in the fusion–fission steady state. It does remain possible that some of the large mitochondrial structures actually result from the clustering of many small, fragmented mitochondria that are not resolved individually by our methods. The rescue of mitochondrial defects in *PINK1* loss-of-function mutants by Parkin overexpression suggests that Parkin is indeed acting downstream of PINK1 in a regulatory pathway, as indicated by genetic studies (Clark et al., 2006; Park et al., 2006). In addition, we overexpressed the yeast alternative NADH oxidoreductase Ndi1p (NDI1) (Vilain et al., 2012) to determine whether the abnormal mitochondrial morphology in motor CBs in the mutants could have resulted from more discrete functional defects in electron transport chain (ETC) complex I, rather than overall organelle senescence. Partial rescue of mitochondrial morphology in motor CBs of *PINK1* mutants by NDI1 OE indicates that ETC complex I functional defects could underlie the morphological changes (Fig. 6Av,Ax,B).

Discussion

Mitochondria are semiautonomous organelles with a complex, incompletely understood pattern of biogenesis, reorganization, and turnover. This is complicated further in neurons by the requirement of mitochondrial transport and redistribution over long distances, which may separate, in time and space, events that are closely coordinated in cells of more modest dimensions. However, a coherent model of mitochondrial turnover in neurons (and its potential failures in neurodegenerative disease) has arisen from studies involving PINK1/Parkin pathway. This pathway, whose compromise produces mitochondrial structural and functional defects in *Drosophila* muscle (Clark et al., 2006; Park et al., 2006; Morais et al., 2009), has been shown to target mitochondria for turnover in cells treated with uncouplers (Matsuda et al., 2010; Narendra et al., 2010). In addition, PINK1 has been proposed to play a regulatory role in axonal mitochondrial motility, by targeting the motor-organelle linker protein Miro for degradation and thus halting the transport of dysfunctional mitochondria (Wang et al., 2011). If these model mechanisms are broadly valid in the complex environment of the nervous system, then they generate several specific phenotypic predictions. We have tested those predictions *in vivo*, by quantitatively determining mitochondrial membrane potential, density, motility behavior, and morphology within the *Drosophila* larval nervous system in *PINK1* deletion mutants. Our findings suggest that PINK1 is required to maintain the normal mitochondrial metabolic state and transport in axons, and for normal morphology in the CB, but not for regulating mitochondrial fusion, or turnover in axons.

Mitochondrial quality control does not show the expected signs of impairment in axons of *PINK1* deletion mutants
If the PINK1 pathway is responsible for the turnover of senescent, depolarized mitochondria, then we expect mitochondria with lower IMP to accumulate in axons of the PINK1-deficient
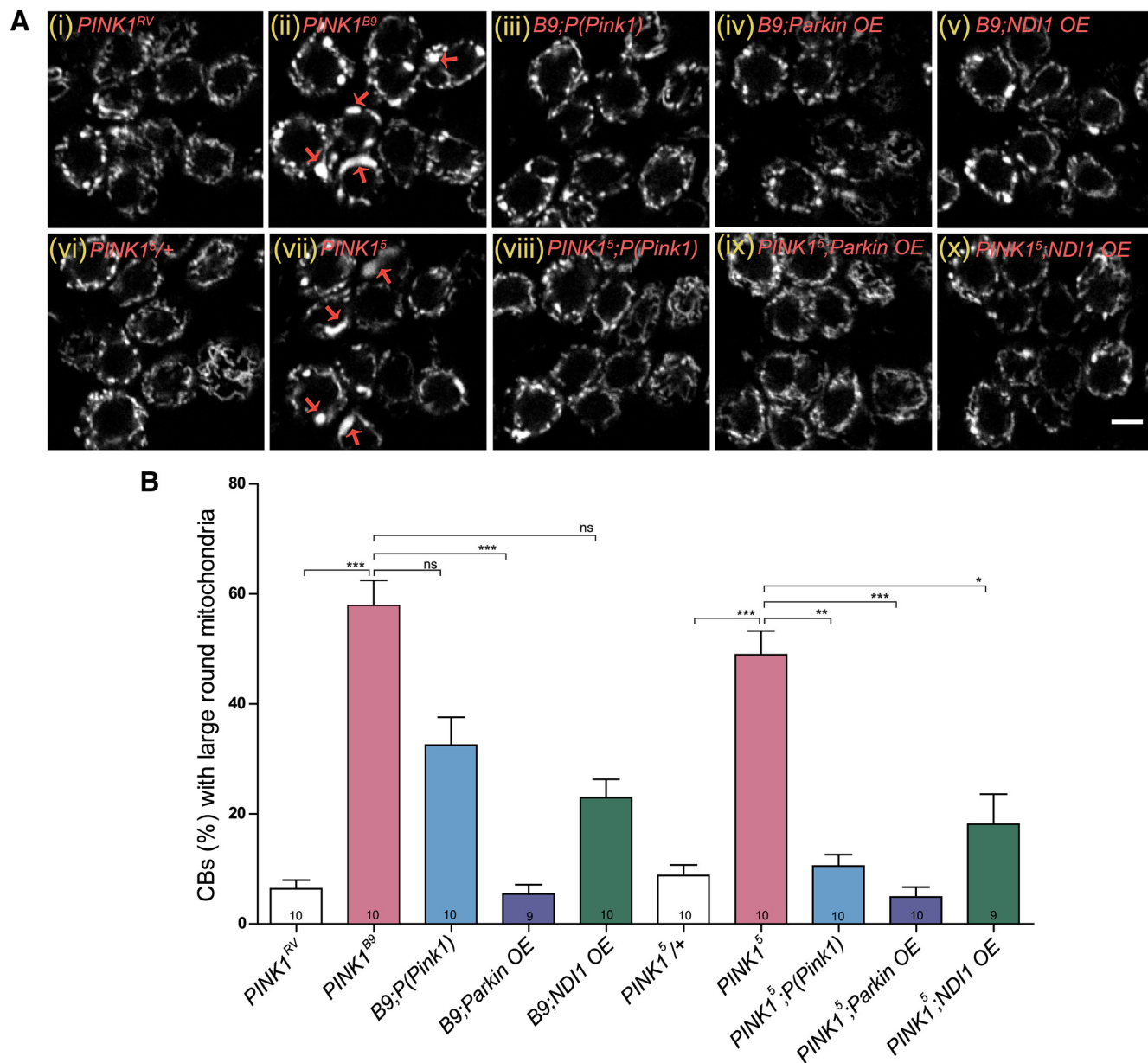
Figure 6. *PINK1* mutants show abnormal mitochondrial morphology in motor neuron CBs. ***A***, Images show mitochondrial morphology in motor neuron CBs of ventral ganglion in *PINK1^{RV}* as control (***i***), *PINK1^{B9}* (***ii***), *PINK1^{B9}*;*P(Pink1)* (genomic rescue) (***iii***), *PINK1^{B9}*;*Parkin OE* (***iv***), *PINK1^{B9}*;*NDI1 OE* (***v***), *PINK1^5/+* as control (***vi***) for *PINK1^5* mutants (***vii***), *PINK1^5*;*P(Pink1)* (genomic rescue) (***viii***), *PINK1^5*;*Parkin OE* (***ix***), and *PINK1^5*;*NDI1 OE* (***x***). Arrows in *PINK1^{B9}* and *PINK1^5* mutants indicate abnormal, rounded mitochondria, in contrast to interconnected, reticular mitochondria in *PINK1^{RV}* and *PINK1^5/+* controls. Scale bar, 5 μm. ***B***, CBs (%) with abnormal, large round mitochondria were quantified for *PINK1^{RV}*, *PINK1^{B9}*, *PINK1^{B9}*;*P(Pink1)* (genomic rescue), *PINK1^{B9}*;*Parkin OE* and *PINK1^{B9}*;*NDI1 OE* and for *PINK1^5/+*, *PINK1^5*, *PINK1^5*;*P(Pink1)* (genomic rescue), *PINK1^5*;*Parkin OE* and *PINK1^5*;*NDI1 OE*. The mitochondrial morphology phenotype observed in *PINK1* loss-of-function mutants was rescued by the expression of genomic levels of P(Pink1) or by Parkin OE or by yeast alternative NADH oxidoreductase Ndi1P OE (NDI1 OE). Number of larvae analyzed is shown on each bar. Error bars indicate SEM. $*p < 0.05$, $**p < 0.01$, $***p < 0.001$ (nonparametric Kruskal–Wallis test with Dunn's post-test). ns, Nonsignificant difference.

nervous system. The effect on IMP could manifest as a general diminution of the mean IMP of the mitochondrial population or as a distinct outlying population with a significantly lower IMP. We observed the former (a modest reduction in IMP of the axonal mitochondrial population overall) and not the latter (Fig. 1). This is consistent in part with the proposed role of PINK1 in turnover and may reflect a protracted failure to cull neuronal mitochondria, whereas the appearance of a distinct outlying population with low IMP might be expected after short-term, acute PINK1 suppression. However, if senescent mitochondria accumulate in the axons of PINK1-deficient neurons, as predicted, then this should also have been appar-

ent as both an increased density of mitochondria and a net diminution of their retrieval to the CB via retrograde transport. We observed neither of these: axonal organelle density remain unchanged (Fig. 4A), and the changes in retrograde traffic were almost exactly balanced by those of anterograde (Fig. 2B,C).

In addition, it is notable that senescent mitochondria should manifest themselves as a small subpopulation with large IM depolarization, to be recognized and tagged by PINK1 for turnover. However, this study and others (Verburg and Hollenbeck, 2008) have found that, under normal physiological conditions, neurons display a striking lack of variation in IMP among the mitochon-

dria within a cell, and there is certainly no evidence for a small outlying population with low IMP. Even in *Drosophila* neurodegenerative disease models, only animals with severe dying-back neuropathy displayed gross depolarization of axonal mitochondria (Shidara and Hollenbeck, 2010). Also, in contrast to the localization of PINK1/Parkin onto majority of mitochondria reported in non-neuronal cells treated with uncouplers (Matsuda et al., 2010; Narendra et al., 2010), studies in neurons found that Parkin is targeted to only a small fraction of depolarized mitochondria after photodamage or drug treatment (Ashrafi et al., 2014). Indeed, recent data show that this discrepancy in Parkin recruitment in neuronal versus non-neuronal cells can be attributed to neuronal bioenergetics, as neurons rely mainly on mitochondrial respiration (Van Laar et al., 2011). Along with our data, this argues against a role for the PINK1 pathway in axonal mitochondrial turnover *in vivo*.

An additional major proposed role of the PINK1 pathway in mitochondrial quality control is the regulation of the fission–fusion steady-state. Downregulation of Mitofusin has been shown to restore the mitochondrial structural defects in *Drosophila* muscle (Poole et al., 2008). Moreover, higher Mitofusin levels were detected in the PINK1-deficient tissue (Poole et al., 2010; Ziviani et al., 2010). Thus, it has been hypothesized that PINK1 targets the Mitofusin of depolarized mitochondria for degradation, thus preventing fusion of senescent, low IMP mitochondria with other, fully functional neighbors (Poole et al., 2010), thereby preserving the health of the population. Any imbalance of mitochondrial fusion–fission processes in axons will be apparent in mitochondrial morphology, as either longer mitochondria due to excessive fusion or small fragmented mitochondria due to higher rates of fission (Amiri and Hollenbeck, 2008; Cagalinec et al., 2013). Thus, *PINK1* mutants should display increased mitochondrial length, either as a change in the population mean or as an outlying, longer senescent population. Here, too, we found no evidence for this prediction *in vivo*: the mean mitochondrial lengths between normal and *PINK1* mutant axons were identical for both moving and stationary organelles, and there was no outlying longer population in the absence of PINK1 (Fig. 5E).

Location of mitochondrial turnover

Although loss of PINK1 function does not affect mitochondrial morphology in motor axons, it is important to recognize that mitochondrial fusion–fission processes, and quality control, probably occurs rarely in axons (Berman et al., 2009; Cagalinec et al., 2013). Despite clear evidence of axonal mitochondrial turnover in embryonic neurons in culture (Maday et al., 2012), it remains likely that much of the mitochondrial processing in the intact nervous system actually occurs in the somatic compartment (Cai et al., 2012). In this case, we would expect PINK1 deficiency to produce a phenotype not in axons, but mainly in the CBs. We did indeed observe that PINK1-deficient CBs frequently contained large, rounded, abnormal mitochondria that are rarely seen in the normal nervous system (Fig. 6). This could reflect defects in biogenesis, fission–fusion, or turnover. Similar mitochondrial morphology has been reported in adult *Drosophila* dopaminergic neurons of *PINK1* mutants, well before the stage of neuronal degeneration (Park et al., 2006). Moreover, the rescue of mitochondrial morphology by yeast NDI1 OE in larval motor neurons that we observe, or by mitochondrial SOD2 overexpression in adult dopaminergic neurons of *PINK1* deletion mutants (Park et al., 2006; Koh et al., 2012), argues for a connection between mitochondrial function and underlying morphological changes. It was notable, however, that, in the absence of PINK1,

we did not observe the predicted increase in mitochondrial volume in CBs, which would result from defective turnover. Along with these data, the reduced entry of anterograde mitochondria into axons in mutants argues for a PINK1 role in mitochondrial biogenesis in the CB, possibly by interacting with the Parkin-PARIS(ZNF746)-PGC-1α pathway (Shin et al., 2011).

Another proposed mechanism for PINK1-dependent mitochondrial quality control that is consistent with our *in vivo* data is one by which organelle components are repaired or replaced piecemeal, as required. Recent studies suggest a role for PINK1 in the maintenance of ETC complex I activity (Morais et al., 2009, 2014; Vilain et al., 2012). Moreover, the complex I deficits in *Drosophila PINK1* mutants are rescued by overexpression of the mitochondrial chaperone TRAP1 (Costa et al., 2013; Zhang et al., 2013). Furthermore, PINK1/Parkin have been shown to be involved in the selective elimination of damaged mitochondrial ETC proteins (Vincow et al., 2013) (Fig. 6). Thus, in neurons it is possible that the PINK1/Parkin pathway preserves mitochondrial function upstream of a role in overall mitochondrial turnover. This could include the maintenance of normal metabolism and ATP production, the failure of which could explain many aspects of the PINK1-deficient phenotypes we observe *in vivo*. We suggest that mitochondrial turnover via tagging and digestion of senescent organelles may be rare in mature axons. In this context, it is worth noting the recent *in vivo* evidence that axonal mitochondria can be degraded in adjacent glial cells following axonal evulsion (Davis et al., 2014).

Manipulation of the PINK1 pathway fails to control the stationary-motile balance in the axon

A hypothesized mechanism for regulating axonal mitochondrial motility proposes that PINK1 tags mitochondria with low IMP to then induce degradation of their motor-organelle linker, Miro (Wang et al., 2011). If so, then we expect *PINK1* mutants to show enhanced anterograde transport and reduced pause times, whereas PINK1 OE should reduce anterograde movement or cause complete cessation of movement. Indeed, we observe the opposite: *PINK1* mutation increases the pause times of anterograde mitochondria and also decreases the velocities of retrograde mitochondria, whereas PINK1 OE actually increases retrogradely moving mitochondria, however, leaving anterograde mitochondria unaffected. Thus, our analysis of mitochondrial motility suggests that PINK1 has a role in mediating the specific motility behaviors of both anterograde and retrograde mitochondria. It is possible that our use of *PINK1*-null mutants, rather than a *PINK1 RNAi* line (Wang et al., 2011; Liu et al., 2012), could account for different findings in mitochondrial motility. Because PINK1 OE is reported to completely halt motility in CCAP neurons (Wang et al., 2011), but not in motor neurons (Fig. 3C) (Liu et al., 2012), it is also possible that PINK1 OE produces neuronal cell type-specific phenotypes. It is also notable that, in all reports, disruption of normal PINK1 levels affected not just anterograde motility, but also retrograde. Indeed, many studies of the modulation of axonal transport also show that experimental interventions ostensibly targeted at one direction of movement actually yield effects on both directions (e.g., Pilling et al., 2006; Morfini et al., 2009; Pigino et al., 2009; Russo et al., 2009; Morfini et al., 2013). Thus, the mechanisms of axonal transport regulation are complex and do not seem to involve a general PINK1-induced halting of anterograde traffic *in vivo*.

In conclusion, our findings indicate that PINK1 is required for normal mitochondrial function and bidirectional axonal transport, but not for mitochondrial turnover or fission–fusion con-

trol in axons *in vivo*. Thus, our results support the idea that mitochondrial turnover and fission–fusion in axons are organized differently *in vivo*, in an intact nervous system, than they are *in vitro*, in neuronal culture. However, PINK1 is required for the maintenance of a normal mitochondrial network in the soma *in vivo*, suggesting that it plays a role there in organelle biogenesis and/or fission–fusion processes.

References

Amiri M, Hollenbeck PJ (2008) Mitochondrial biogenesis in the axons of vertebrate peripheral neurons. Dev Neurobiol 68:1348–1361. CrossRef Medline

Ashrafi G, Schwarz TL (2013) The pathways of mitophagy for quality control and clearance of mitochondria. Cell Death Differ 20:31–42. CrossRef Medline

Ashrafi G, Schlehe JS, LaVoie MJ, Schwarz TL (2014) Mitophagy of damaged mitochondria occurs locally in distal neuronal axons and requires PINK1 and Parkin. J Cell Biol 206:655–670. CrossRef Medline

Baloh RH, Schmidt RE, Pestronk A, Milbrandt J (2007) Altered axonal mitochondrial transport in the pathogenesis of Charcot-Marie-Tooth disease from mitofusin 2 mutations. J Neurosci 27:422–430. CrossRef Medline

Berman SB, Chen YB, Qi B, McCaffery JM, Rucker EB 3rd, Goebbels S, Nave KA, Arnold BA, Jonas EA, Pineda FJ, Hardwick JM (2009) Bcl-x L increases mitochondrial fission, fusion, and biomass in neurons. J Cell Biol 184:707–719. CrossRef Medline

Bolte S, Cordelières FP (2006) A guided tour into subcellular colocalization analysis in light microscopy. J Microsc 224:213–232. CrossRef Medline

Cagalinec M, Safiulina D, Liiv M, Liiv J, Choubey V, Wareski P, Veksler V, Kaasik A (2013) Principles of the mitochondrial fusion and fission cycle in neurons. J Cell Sci 126:2187–2197. CrossRef Medline

Cai Q, Zakaria HM, Simone A, Sheng ZH (2012) Spatial Parkin translocation and degradation of damaged mitochondria via mitophagy in live cortical neurons. Curr Biol 22:545–552. CrossRef Medline

Chada SR, Hollenbeck PJ (2003) Mitochondrial movement and positioning in axons: the role of growth factor signaling. J Exp Biol 206:1985–1992. CrossRef Medline

Chada SR, Hollenbeck PJ (2004) Nerve growth factor signaling regulates motility and docking of axonal mitochondria. Curr Biol 14:1272–1276. CrossRef Medline

Chang DT, Reynolds IJ (2006) Mitochondrial trafficking and morphology in healthy and injured neurons. Prog Neurobiol 80:241–268. CrossRef Medline

Chen H, Chan DC (2009) Mitochondrial dynamics—fusion, fission, movement, and mitophagy—in neurodegenerative diseases. Hum Mol Genet 18:R169–R176. CrossRef Medline

Clark IE, Dodson MW, Jiang C, Cao JH, Huh JR, Seol JH, Yoo SJ, Hay BA, Guo M (2006) *Drosophila* Pink1 is required for mitochondrial function and interacts genetically with parkin. Nature 441:1162–1166. CrossRef Medline

Costa AC, Loh SH, Martins LM (2013) *Drosophila* Trap1 protects against mitochondrial dysfunction in a PINK1/parkin model of Parkinson's disease. Cell Death Dis 4:e467. CrossRef Medline

Davis CH, Kim KY, Bushong EA, Mills EA, Boassa D, Shih T, Kinebuchi M, Phan S, Zhou Y, Bihlmeyer NA, Nguyen JV, Jin Y, Ellisman MH, Marsh-Armstrong N (2014) Transcellular degradation of axonal mitochondria. Proc Natl Acad Sci U S A 111:9633–9638. CrossRef Medline

Devireddy S, Sung H, Liao PC, Garland-Kuntz E, Hollenbeck PJ (2014) Analysis of mitochondrial traffic in *Drosophila*. Methods Enzymol 547:131–150. CrossRef Medline

Gautier CA, Kitada T, Shen J (2008) Loss of PINK1 causes mitochondrial functional defects and increased sensitivity to oxidative stress. Proc Natl Acad Sci U S A 105:11364–11369. CrossRef Medline

Hollenbeck PJ (2005) Mitochondria and neurotransmission: evacuating the synapse. Neuron 47:331–333. CrossRef Medline

Hollenbeck PJ, Saxton WM (2005) The axonal transport of mitochondria. J Cell Sci 118:5411–5419. CrossRef Medline

Hollenbeck PJ, Bray D, Adams RJ (1985) Effects of the uncoupling agents FCCP and CCCP on the saltatory movements of cytoplasmic organelles. Cell Biol Int Rep 9:193–199. CrossRef Medline

Koh H, Kim H, Kim MJ, Park J, Lee HJ, Chung J (2012) Silent information

regulator 2 (Sir2) and Forkhead box O (FOXO) complement mitochondrial dysfunction and dopaminergic neuron loss in *Drosophila* PTEN-induced kinase 1 (PINK1) null mutant. J Biol Chem 287:12750–12758. CrossRef Medline

Liu S, Sawada T, Lee S, Yu W, Silverio G, Alapat P, Millan I, Shen A, Saxton W, Kanao T, Takahashi R, Hattori N, Imai Y, Lu B (2012) Parkinson's disease-associated kinase PINK1 regulates Miro protein level and axonal transport of mitochondria. PLoS Genet 8:e1002537. CrossRef Medline

Louie K, Russo GJ, Salkoff DB, Wellington A, Zinsmaier KE (2008) Effects of imaging conditions on mitochondrial transport and length in larval motor axons of *Drosophila*. Comp Biochem Physiol A Mol Integr Physiol 151:159–172. CrossRef Medline

Maday S, Wallace KE, Holzbaur EL (2012) Autophagosomes initiate distally and mature during transport toward the cell soma in primary neurons. J Cell Biol 196:407–417. CrossRef Medline

Matsuda N, Sato S, Shiba K, Okatsu K, Saisho K, Gautier CA, Sou YS, Saiki S, Kawajiri S, Sato F, Kimura M, Komatsu M, Hattori N, Tanaka K (2010) PINK1 stabilized by mitochondrial depolarization recruits Parkin to damaged mitochondria and activates latent Parkin for mitophagy. J Cell Biol 189:211–221. CrossRef Medline

Miller KE, Sheetz MP (2004) Axonal mitochondrial transport and potential are correlated. J Cell Sci 117:2791–2804. CrossRef Medline

Misko A, Jiang S, Wegorzewska I, Milbrandt J, Baloh RH (2010) Mitofusin 2 is necessary for transport of axonal mitochondria and interacts with the Miro/Milton Complex. J Neurosci 30:4232–4240. CrossRef Medline

Morais VA, Verstreken P, Roethig A, Smet J, Snellinx A, Vanbrabant M, Haddad D, Frezza C, Mandemakers W, Vogt-Weisenhorn D, Van Coster R, Wurst W, Scorrano L, De Strooper B (2009) Parkinson's disease mutations in PINK1 result in decreased Complex I activity and deficient synaptic function. EMBO Mol Med 1:99–111. CrossRef Medline

Morais VA, Haddad D, Craessaerts K, De Bock PJ, Swerts J, Vilain S, Aerts L, Overbergh L, Grünewald A, Seibler P, Klein C, Gevaert K, Verstreken P, De Strooper B (2014) PINK1 loss-of-function mutations affect mitochondrial complex I activity via NdufA10 ubiquinone uncoupling. Science 344:203–207. CrossRef Medline

Morfini GA, You YM, Pollema SL, Kaminska A, Liu K, Yoshioka K, Björkblom B, Coffey ET, Bagnato C, Han D, Huang CF, Banker G, Pigino G, Brady ST (2009) Pathogenic huntingtin inhibits fast axonal transport by activating JNK3 and phosphorylating kinesin. Nat Neurosci 12:864–871. CrossRef Medline

Morfini GA, Bosco DA, Brown H, Gatto R, Kaminska A, Song Y, Molla L, Baker L, Marangoni MN, Berth S, Tavassoli E, Bagnato C, Tiwari A, Hayward LJ, Pigino GF, Watterson DM, Huang CF, Banker G, Brown RH Jr, Brady ST (2013) Inhibition of fast axonal transport by pathogenic SOD1 involves activation of p38 MAP kinase. PLoS One 8:e65235. CrossRef Medline

Narendra DP, Jin SM, Tanaka A, Suen DF, Gautier CA, Shen J, Cookson MR, Youle RJ (2010) PINK1 is selectively stabilized on impaired mitochondria to activate Parkin. PLoS Biol 8:e1000298. CrossRef Medline

Ollion J, Cochennec J, Loll F, Escudé C, Boudier T (2013) TANGO: a generic tool for high-throughput 3D image analysis for studying nuclear organization. Bioinformatics 29:1840–1841. CrossRef Medline

Park J, Lee SB, Lee S, Kim Y, Song S, Kim S, Bae E, Kim J, Shong M, Kim JM, Chung J (2006) Mitochondrial dysfunction in *Drosophila* PINK1 mutants is complemented by parkin. Nature 441:1157–1161. CrossRef Medline

Pathak D, Sepp KJ, Hollenbeck PJ (2010) Evidence that Myosin activity opposes microtubule-based axonal transport of mitochondria. J Neurosci 30:8984–8992. CrossRef Medline

Pigino G, Morfini G, Atagi Y, Deshpande A, Yu C, Jungbauer L, LaDu M, Busciglio J, Brady S (2009) Disruption of fast axonal transport is a pathogenic mechanism for intraneuronal amyloid beta. Proc Natl Acad Sci U S A 106:5907–5912. CrossRef Medline

Pilling AD, Horiuchi D, Lively CM, Saxton WM (2006) Kinesin-1 and dynein are the primary motors for fast transport of mitochondria in *Drosophila* motor axons. Mol Biol Cell 17:2057–2068. CrossRef Medline

Poole AC, Thomas RE, Andrews LA, McBride HM, Whitworth AJ, Pallanck LJ (2008) The PINK1/Parkin pathway regulates mitochondrial morphology. Proc Natl Acad Sci U S A 105:1638–1643. CrossRef Medline

Poole AC, Thomas RE, Yu S, Vincow ES, Pallanck L (2010) The mitochondrial fusion-promoting factor Mitofusin is a substrate of the PINK1/Parkin pathway. PLoS One 5:e10054. CrossRef Medline

Rintoul GL, Filiano AJ, Brocard JB, Kress GJ, Reynolds IJ (2003) Glutamate decreases mitochondrial size and movement in primary forebrain neurons. J Neurosci 23:7881–7888. Medline

Rugarli EI, Langer T (2012) Mitochondrial quality control: a matter of life and death for neurons. EMBO J 31:1336–1349. CrossRef Medline

Russo GJ, Louie K, Wellington A, Macleod GT, Hu F, Panchumarthi S, Zinsmaier KE (2009) *Drosophila* Miro is required for both anterograde and retrograde axonal mitochondrial transport. J Neurosci 29:5443–5455. CrossRef Medline

Saxton WM, Hollenbeck PJ (2012) The axonal transport of mitochondria. J Cell Sci 125:2095–2104. CrossRef Medline

Scaduto RC Jr, Grotyohann LW (1999) Measurement of mitochondrial membrane potential using fluorescent rhodamine derivatives. Biophys J 76:469–477. CrossRef Medline

Shidara Y, Hollenbeck PJ (2010) Defects in mitochondrial axonal transport and membrane potential without increased reactive oxygen species production in a *Drosophila* model of Friedreich ataxia. J Neurosci 30:11369–11378. CrossRef Medline

Shin JH, Ko HS, Kang H, Lee Y, Lee YI, Pletinkova O, Troconso JC, Dawson VL, Dawson TM (2011) PARIS (ZNF746) repression of PGC-1α contributes to neurodegeneration in Parkinson's disease. Cell 144:689–702. CrossRef Medline

Siegel S, Castellan NJ (1988) Nonparametric statistics for the behavioral sciences, Ed 2. New York: McGraw-Hill.

Thevenaz P, Ruttimann UE, Unser M (1998) A pyramid approach to subpixel registration based on intensity. IEEE T Image Process 7:27–41. CrossRef Medline

Van Laar VS, Arnold B, Cassady SJ, Chu CT, Burton EA, Berman SB (2011) Bioenergetics of neurons inhibit the translocation response of Parkin following rapid mitochondrial depolarization. Hum Mol Genet 20:927–940. CrossRef Medline

Verburg J, Hollenbeck PJ (2008) Mitochondrial membrane potential in axons increases with local nerve growth factor or semaphorin signaling. J Neurosci 28:8306–8315. CrossRef Medline

Verstreken P, Ly CV, Venken KJ, Koh TW, Zhou Y, Bellen HJ (2005) Synaptic mitochondria are critical for mobilization of reserve pool vesicles at *Drosophila* neuromuscular junctions. Neuron 47:365–378. CrossRef Medline

Vilain S, Esposito G, Haddad D, Schaap O, Dobreva MP, Vos M, Van Meensel S, Morais VA, De Strooper B, Verstreken P (2012) The yeast complex I equivalent NADH dehydrogenase rescues pink1 mutants. PLoS Genet 8:e1002456. CrossRef Medline

Vincow ES, Merrihew G, Thomas RE, Shulman NJ, Beyer RP, MacCoss MJ, Pallanck LJ (2013) The PINK1-Parkin pathway promotes both mitophagy and selective respiratory chain turnover in vivo. Proc Natl Acad Sci U S A 110:6400–6405. CrossRef Medline

Wang X, Winter D, Ashrafi G, Schlehe J, Wong YL, Selkoe D, Rice S, Steen J, LaVoie MJ, Schwarz TL (2011) PINK1 and Parkin target Miro for phosphorylation and degradation to arrest mitochondrial motility. Cell 147:893–906. CrossRef Medline

Youle RJ, Narendra DP (2011) Mechanisms of mitophagy. Nat Rev Mol Cell Biol 12:9–14. CrossRef Medline

Zhang L, Karsten P, Hamm S, Pogson JH, Müller-Rischart AK, Exner N, Haass C, Whitworth AJ, Winklhofer KF, Schulz JB, Voigt A (2013) TRAP1 rescues PINK1 loss-of-function phenotypes. Hum Mol Genet 22:2829–2841. CrossRef Medline

Ziviani E, Tao RN, Whitworth AJ (2010) *Drosophila* Parkin requires PINK1 for mitochondrial translocation and ubiquitinates Mitofusin. Proc Natl Acad Sci U S A 107:5018–5023. CrossRef Medline